Supplementary Information

Rapid Self-Healing Glassy Polymer/Metal-Organic-Framework **Hybrid Membrane at Room Temperature**

Qingyu Niu, Hang Han, Xiao Liu, Bin Li, Huanrong Li and Zhiqiang Li*

Tianjin Key Laboratory of Chemical Process Safety, School of Chemical Engineering and Technology, Hebei University of Technology, Tianjin 300130, P. R. China

*Corresponding Authors: zhiqiangli@hebut.edu.cn

Contents

1. Experimental Methods

Materials

All chemicals were used without further purification unless noted otherwise. Acrylamide (AAm) was purchased from J&K Scientific Ltd., Beijing, China. Methanol (99.9%), $TbCl_3 \cdot 6H_2O$ (99.99%) and $EuCl_3 \cdot 6H_2O$ (99.99%) was purchased from Beijing HWRK Chem Co., Ltd.

Characterization

^1H NMR spectra were recorded on a Bruker 400 instrument. FTIR spectra were obtained on a Bruker Vector 22 spectrometer in the range of 400-4000 cm^{-1} at a resolution of 4 cm^{-1} (16 scans were collected). Temperature-dependent FTIR spectra were obtained on a Tensor 27 instrument. The polyLnMOF-RHP was heated from 20 °C to 150 °C at 1 °C/min, and the temperature-dependent FTIR spectra were collected at the same time. Moreover, we collected 21 spectra (from 20 °C to 40 °C at the heating rate of 1 °C/min) and used 2DCS software to process these data, generating the generalized 2D correlation spectra. The ^1H NMR curves with different temperatures were measured on Bruker AVANCE III TM HD 500 MHz spectrometer with DMSO-d_6 as solvent. Powder X-ray diffraction (PXRD) analyses were carried on a Bruker D8 Discover. Differential scanning calorimetry (DSC) tests were performed on a Perkin Elmer Diamond DSC with the mass of all samples ranging from 6 mg to 10 mg. Samples were heated from -50 °C to 150 °C with heating rate of 10 °C/min and then cooling to -50 °C at 10 °C/min. And the heating and cooling processes were performed two times. Dynamic mechanical analysis (DMA) tests were measured on Tritec 2000 in a tension mode with the sample dimension about 20 × 5 × 1 mm^3. And tests were performed in temperature scanning mode in the range of -20 °C to 70 °C at a ramping rate of 3 °C/min and a frequency of 1 Hz with a strain amplitude of 30 μm. Thermogravimetric analysis (TGA) was carried out under an N_2 atmosphere from room temperature to 700 °C using a Shimadzu TGA-50 analyzer at a heating rate of 10 °C/min. Tensile properties were determined on CMT6104 with a crosshead speed of 10 mm/min. To measure the self-healing efficiency, the specimen was cut by a razor blade, and the fresh cut surfaces were recombined by hand and then put into vacuum oven at 25 °C for different time. The healed sample was subjected to on stretching experiment again. The steady-state luminescence spectra were measured on an Edinburgh Instruments FS920P near-infrared spectrometer, with a 450 W xenon lamp as the steady-state excitation source, a double excitation monochromator (1800 lines·mm^{-1}), an emission monochromator (600 lines·mm^{-1}), a semiconductor cooled Hamamatsu RMP928 photomultiplier tube. The photoinduced copolymerization was performed under a 500 W Hg lamp. ^{1}H NMR experiment: EuMOF, polyEuMOF and PAAm were firstly digested in DCl (0.1 mL) for 1h, then DMSO-d_6 (0.4 mL) was added. The molecular weight of the RHP were determined by GPC at 40 °C on an Agilent Waters Ultrahydrogel columns with an Agilent RID G1362A detector (0.1mol/L $NaNO_3$ as the eluent). In detail, the polyEuMOF was dissolved in water, then HCl was added to digest the insoluble MOF, and monitored by GPC.

Synthesis of RHP

RHP was prepared by one-pot method through Michael addition reaction between N,N'-methylene diacrylamide (MBA) and 1,4-Butanediamine (BDA) at the molar ratios of 1/1.125.[1] MBA (12.334 g, 0.08 mol) was dissolved in the mixed solvent of 60 mL methanol and 30 mL deionized water. BDA (7.934 g, 0.09 mol) was then dissolved in a mixture of 20 ml methanol and 10 ml deionized water and added directly into the flask. After stirring at 30 °C for 24 h, the solution was poured into a beaker containing 1000 mL of acetone and precipitated at room temperature. The crude product was washed three times with acetone to give solids and then dried in a vacuum oven at 50 °C for 48 h.

Synthesis of EuMOF-RHP$_{80\%}$ hybrid membrane (physical mix)

After dispersing EuMOFs (120 mg) and RHP (480 mg) in methanol, the obtained mixture was dried in a vacuum oven at 50 °C for 24 h. In a typical process, EuMOF-RHP was powdered in a universal crusher, and then hot pressed under 10 MPa at 100

°C for 30 min in the mold to form the EuMOF-$RHP_{80\%}$ hybrid membrane.

Synthesis of PAAm-$RHP_{80\%}$ hybrid membrane

AAm (120 mg, 1.69 mmol) and methanol (2 mL) were added to a centrifuge tube and sonicated for 10 min. After phenylbis(2,4,6-trimethylbenzoyl)phosphine oxide (6 wt% with respect to the weight of the monomer) was added to mixture and sonicated for 2 min. The mixture was photopolymerized under a UV lamp for 50 min to perpare PAAm. After dispersing PAAm (120 mg) and RHP (480 mg) in methanol, the obtained mixture was dried in a vacuum oven at 50 °C for 24 h. In a typical process, PAAm-RHP was powdered in a universal crusher, and then hot pressed under 10 MPa at 100 °C for 30 min in the mold to form the PAAm-$RHP_{80\%}$ hybrid membrane.

Synthesis of EuMOF-PBMA-$RHP_{80\%}$ hybrid membrane

Butyl methacrylate (BMA, 45 mg, 0.32 mmol), EuMOFs (75 mg) and methanol (2 mL) were added to a centrifuge tube and sonicated for 10 min. After phenylbis(2,4,6-trimethylbenzoyl)phosphine oxide (6 wt% with respect to the weight of the monomer) was added to mixture and sonicated for 2 min. The mixture was photopolymerized under a UV lamp for 50 min to perpare polyEuMOF (EuMOF-PBMA). After dispersing the EuMOF-PBMA and RHP (480 mg) in methanol, the obtained mixture was dried in a vacuum oven at 50 °C for 24 h. In a typical process, EuMOF-PBMA-RHP was powdered in a universal crusher, and then hot pressed under 10 MPa at 100 °C for 30 min in the mold to form the EuMOF-PBMA-$RHP_{80\%}$ hybrid membrane.

Theoretical Methods

Healing efficiency (η) is calculated according to the following equation:[1]

$$\eta = \frac{\sigma_{\text{hea}}}{\sigma_{\text{ori}}} \times 100\% \qquad \text{(S1)}$$

where σ_{hea} is the tensile strength of the healing samples, and σ_{ori} is the tensile strength for the original samples.

Energy transfer efficiency (E) between the donor (Tb^{3+}) and the acceptor (Eu^{3+}) is calculated according to the following equation:[2]

$$E = 1 - \frac{\tau_{\mathrm{da}}}{\tau_{\mathrm{d}}} \times 100\% \tag{S2}$$

where τ_{da} and τ_{d} are the luminescence lifetimes of the donor in the presence and absence of the receptor, respectively.

The relative sensitivity (Sr) refers to the relative change of the temperature-sensitive parameter per degree of temperature change, and it is defined as:[3]

$$S_r = \frac{\partial\Delta/\partial T}{\Delta} \tag{S3}$$

where Δ is the measured temperature-sensitive parameter, which indicates $I_{\mathrm{Tb}}/I_{\mathrm{Eu}}$ in this article. T is temperature. The unit of Sr is usually expressed as the percentage change per Kelvin ($\%\cdot K^{-1}$), Sr is often used to compare the performance of different LnMOF thermometers.

The temperature uncertainty (δT) is another parameter to evaluate the thermometer performance. It is defined as the smallest temperature change which can be detected in a given measurement and can be determined by:[4]

$$\delta T = \frac{\delta\Delta/\Delta}{S_r} \tag{S4}$$

where $\delta\Delta/\Delta$ is the relative uncertainty of Δ in determination of the thermometric parameter.

Repeatability refers to the variation of repeated measurements performed under the same conditions and estimated as:[3]

$$R = 1 - \frac{max(|\Delta_c - \Delta_i|)}{\Delta} \tag{S5}$$

where Δ_c is the average temperature measurement parameter extracted from the calibration curve, and Δ_i is each measurement value of the temperature measurement parameter.

2. Supplementary Figures and Tables

Table S1. Recipes of polyEuMOF-RHP with different amount of RHP.

Sample name	polyLnMOF-RHP$_{80\%}$	polyLnMOF-RHP$_{70\%}$	polyLnMOF-RHP$_{60\%}$
$m_{(EuMOF)}$/mg	75	75	75
$m_{(AAm)}$/mg	45	105	165
$m_{(initiator)}$/mg	7.2	10.8	14.4
$m_{(RHP)}$/mg	480	420	380

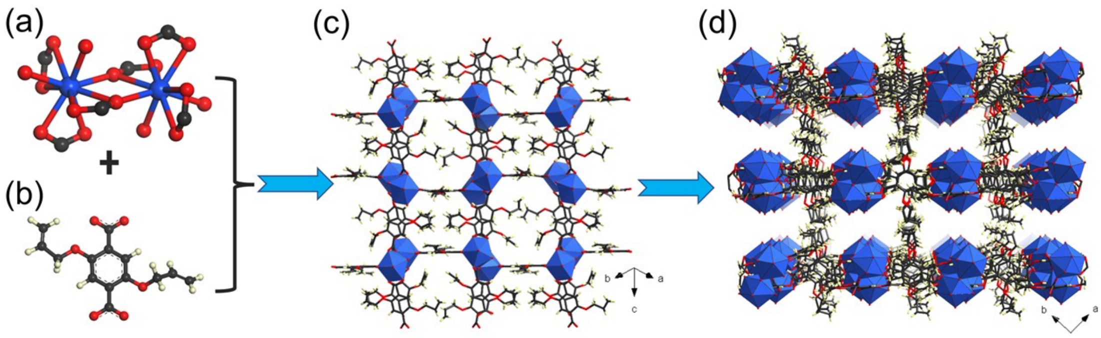

Fig. S1. Single structure of Eu-BABDC showing (a) the coordination environment of the Eu dimeric, and (b) the organic ligand BABDC. (c) The 2D layer structure of Eu-BABDC was constructed by the Eu_2 unit and functional organic ligands. (d) The two-dimensional layer structure was further connected by the interlayer supramolecular interaction to generate a three-dimensional open framework. Eu, O, C, and H atoms are shown as blue, red, gray, and light-yellow spheres, respectively.

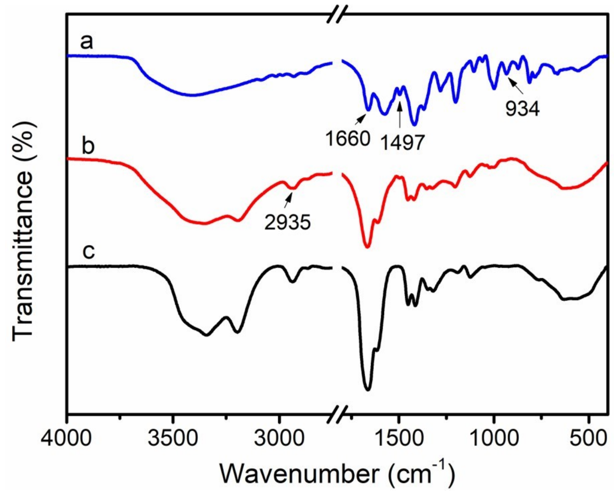

Fig. S2. FTIR spectra of EuMOF (a), polyEuMOF (b) and PAAm (c).

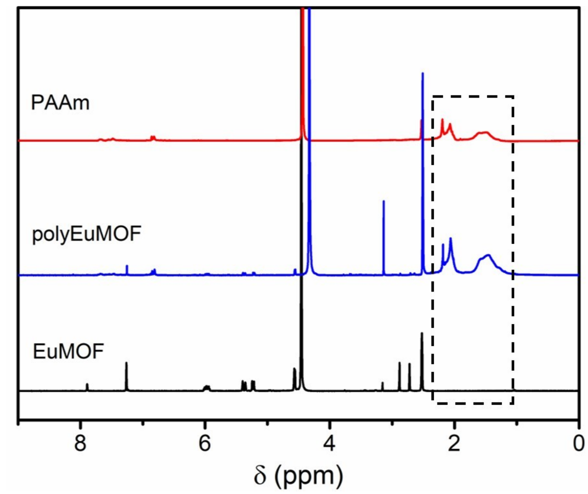

Fig. S3. ^{1}H NMR spectra of EuMOF, polyEuMOF and PAAm in DMSO-d_6/DCl (4:1, v:v).

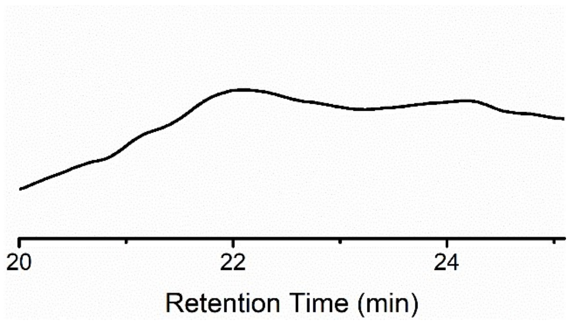

Fig. S4. GPC trace of digested polyEuMOF, from which Mn = 4817 g/mol and Mw = 7389 g/mol was obtained, corresponding to degree of polymerization (DP) 40.6 according to the molar ratio of acrylamide and H_2BABDC. To be noticed, the information was from destroyed fragment peak, rather than accurate polyEuMOF.

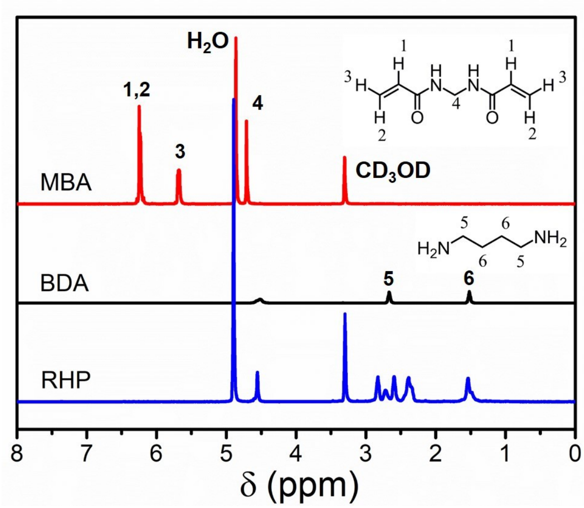

Fig. S5. NMR analysis. [1]H NMR spectra of MBA, BDA and RHP in CD_3OD. The terminal olefin protons signal at 6.24 ppm and 5.69 ppm disappeared after reaction, while new signals appeared at 2-3 ppm belonging to the methylene of -CH_2-CH_2-CONH- in RHP, indicating RHP was successfully synthesized.[5]

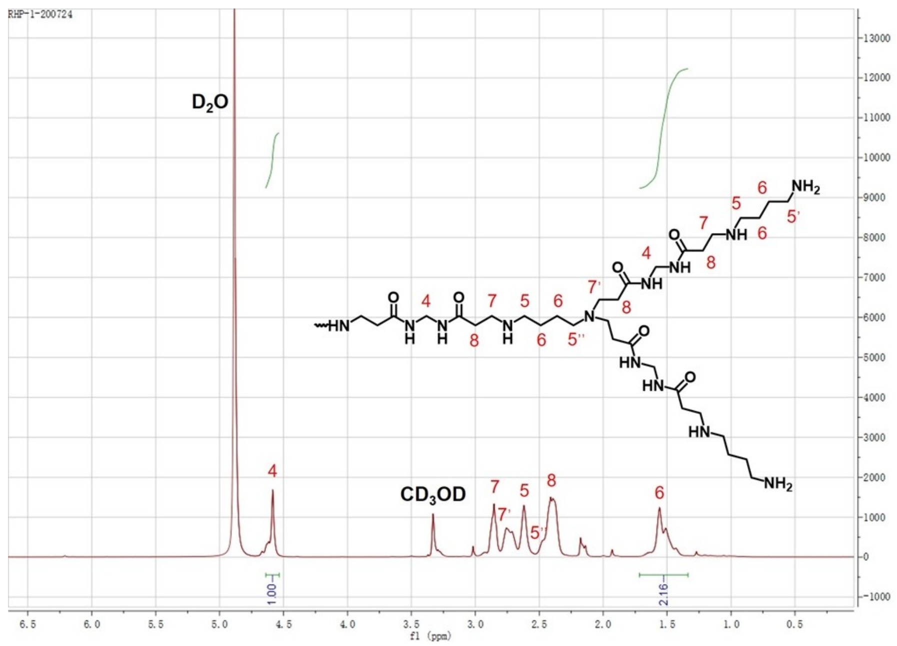

Fig. S6. The Chemical structure and [1]H NMR spectrum of RHP (CD_3OD).

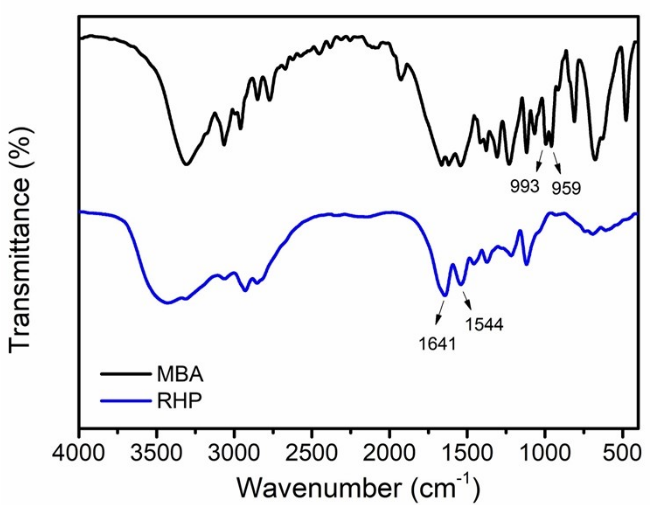

Fig. S7. FTIR analysis. FTIR spectra of MBA and RHP. The vinyl groups bending vibration peaks of MBA at 993 and 959cm^{-1} disappeared and the new peaks assigned to the characteristic amide I band and amide II band occurred at 1641 and 1544 cm^{-1}, demonstrating the successful preparation of RHP.[6]

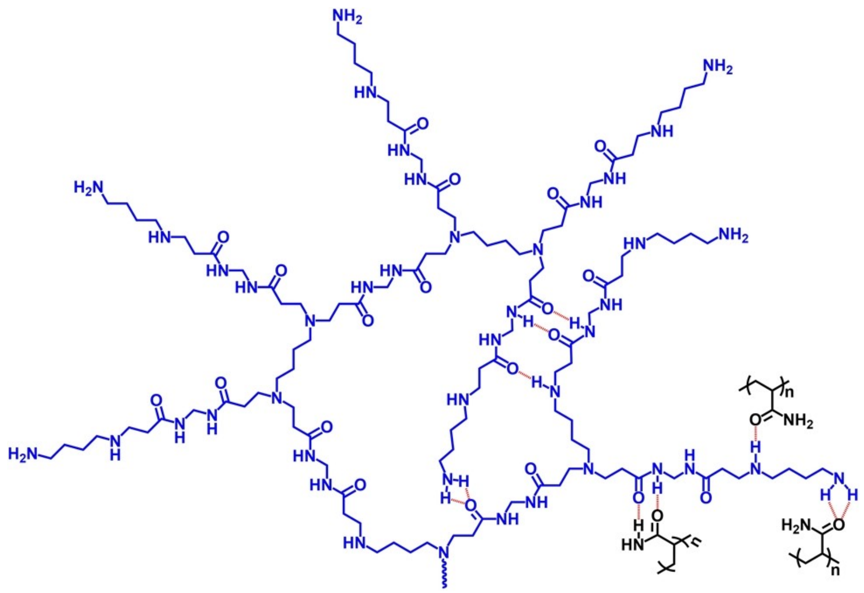

Fig. S8. Chemical structure of the PAAm-RHP interpenetrating network (Red dotted line represents the hydrogen bond).

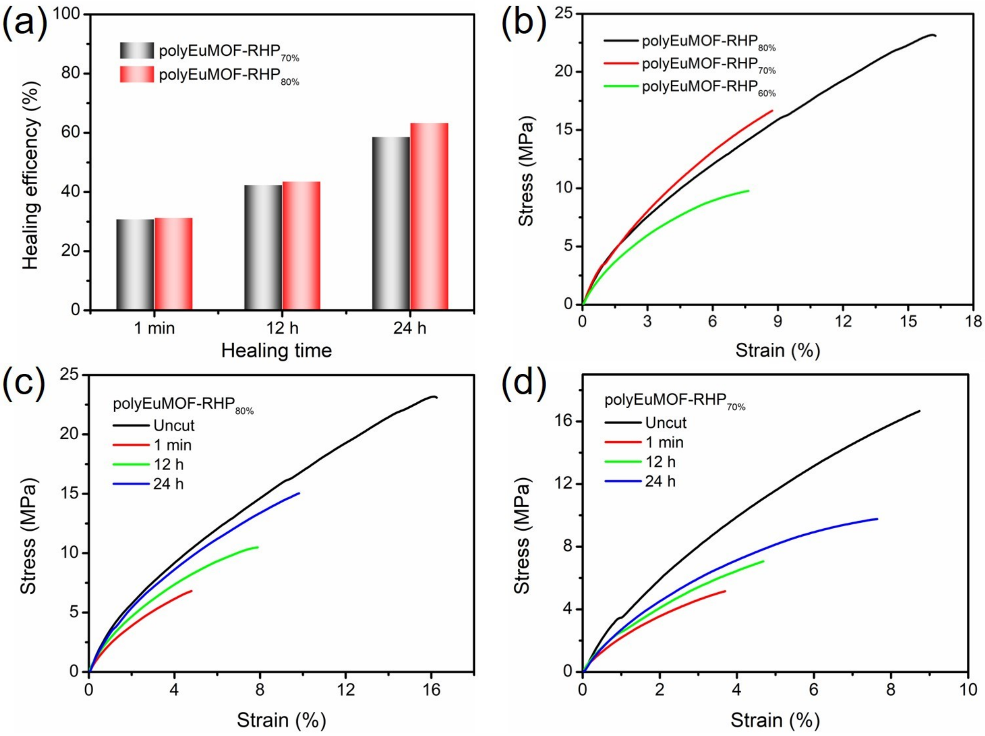

Fig. S9. (a) Self-healing efficiency of the polyEuMOF-RHP membranes with different amount of RHP healed at 25 °C for different time periods. (b) The stress-strain curve of polyEuMOF-RHP. The stress-strain curves of the polyEuMOF-$RHP_{80\%}$ (c) and polyEuMOF-$RHP_{70\%}$ (d) self-healed at 25 °C for different time.

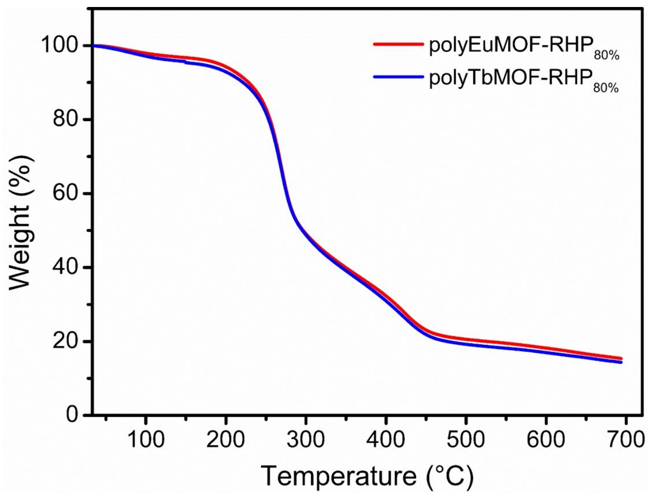

Fig. S10. TG curves of polyEuMOF-$RHP_{80\%}$ and polyTbMOF-$RHP_{80\%}$ membrane.

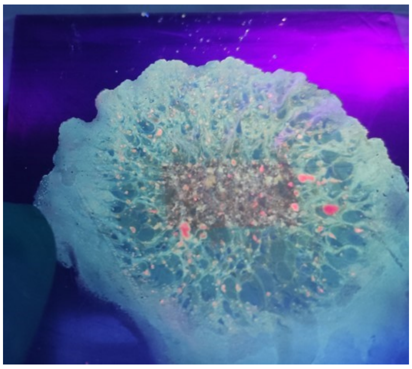

Fig. S11. The photograph of EuMOF-PBMA-RHP$_{80\%}$ membrane under UV light (365 nm).

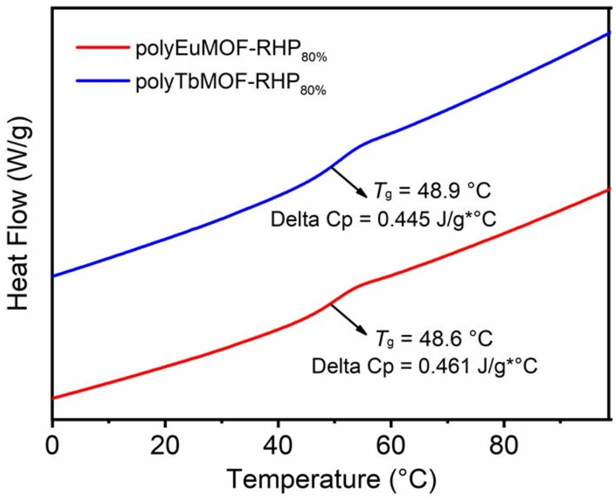

Fig. S12. DSC curves of polyEuMOF-RHP$_{80\%}$ and polyTbMOF-RHP$_{80\%}$ on the second healing time with a healing rate of 10 °C/min.

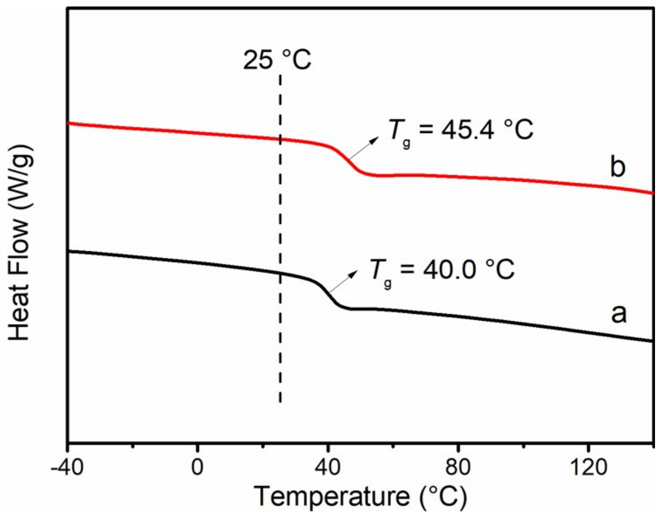

Fig. S13. DSC curves of PAAm-RHP$_{80\%}$ (a) and EuMOF-RHP$_{80\%}$ (b) on the second healing time with a healing rate of 10 °C/min.

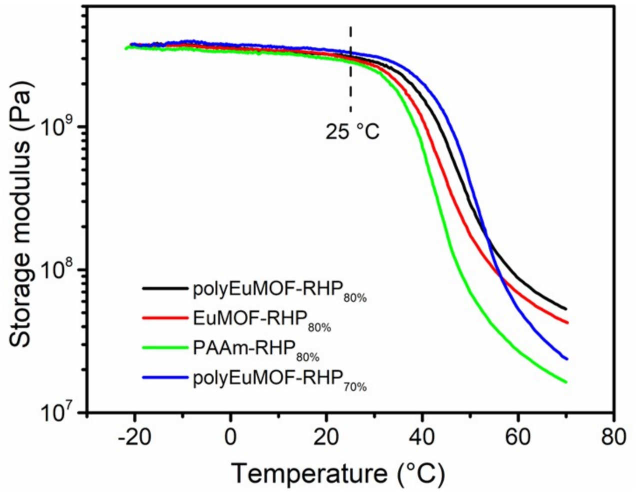

Fig. S14. Temperature dependence of storage modulus of polyEuMOF-RHP$_{80\%}$, EuMOF-RHP$_{80\%}$, PAAm-RHP$_{80\%}$ and polyEuMOF-RHP$_{70\%}$ membrane.

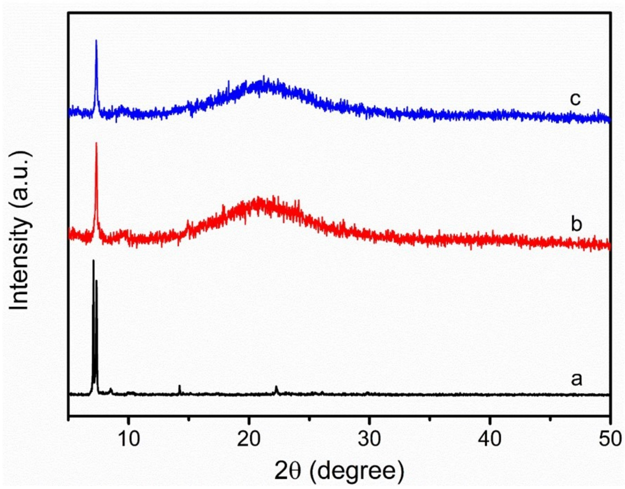

Fig. S15. PXRD patterns of EuMOF (a) and polyEuMOF-RHP$_{80\%}$ membrane before (b) and after self-healing (c).

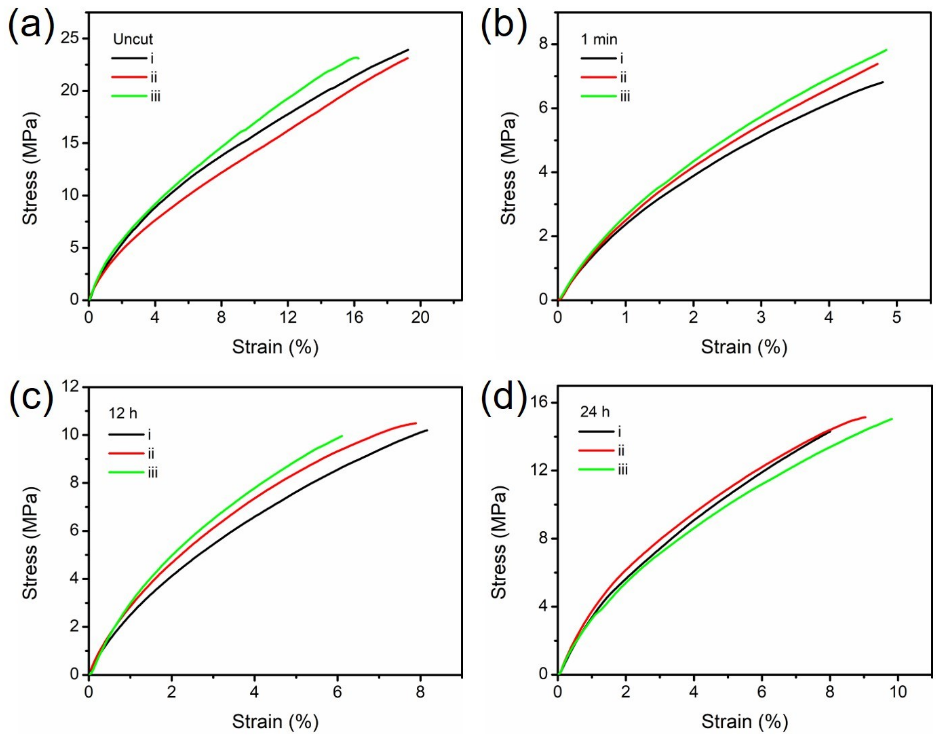

Fig. S16. The stress-strain curves of the polyEuMOF-RHP$_{80\%}$ (a) and self-healed at 25 °C for 1 min (b), 12 h (c) and 24 h (d).

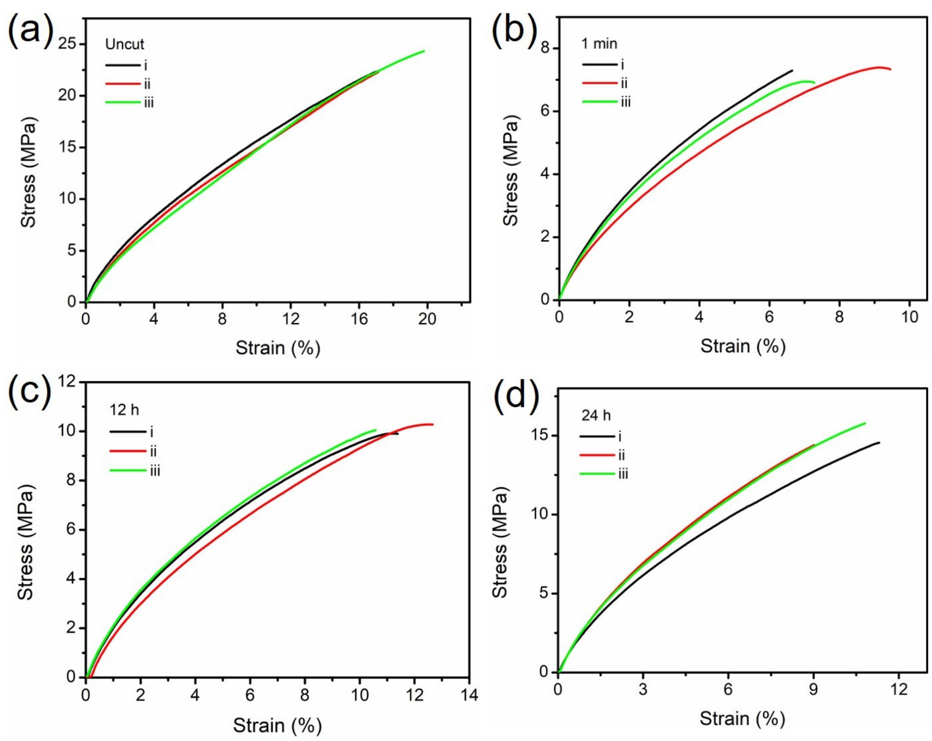

Fig. S17. The stress-strain curves of the polyTbMOF-RHP$_{80\%}$ (a) and self-healed at 25 °C for 1 min (b), 12 h (c) and 24 h (d).

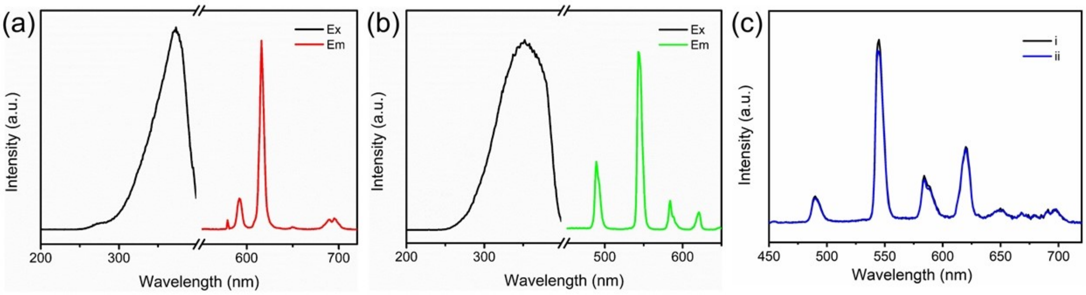

Fig. S18. Excitation (left) and emission (right) spectra of polyEuMOF-RHP$_{80\%}$ (a) and polyTbMOF-RHP$_{80\%}$ (b) membrane at room temperature. (c) Luminescence emission spectra of polyEu$_{0.0025}$Tb$_{0.9975}$MOF-RHP$_{80\%}$ membrane (i) and exposed to high humidity (86% RH, 25 °C, 12 h) (ii).

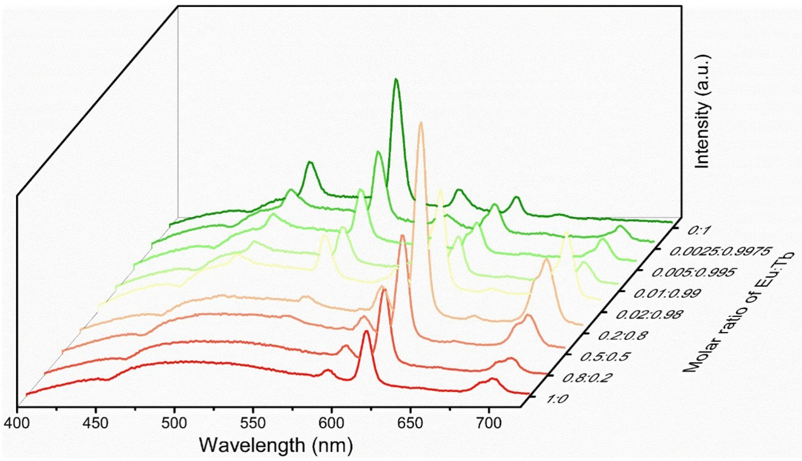

Fig. S19. Luminescence emission spectra of polyLnMOF-RHP$_{80\%}$ membrane with various Eu^{3+}/Tb^{3+} molar ratio (Eu^{3+}/Tb^{3+} = 1:0, 0.8:0.2, 0.5:0.5, 0.2:0.8, 0.02:0.98, 0.01:0.99, 0.005:0.995, 0.0025:0.9975 and 0:1, respectively).

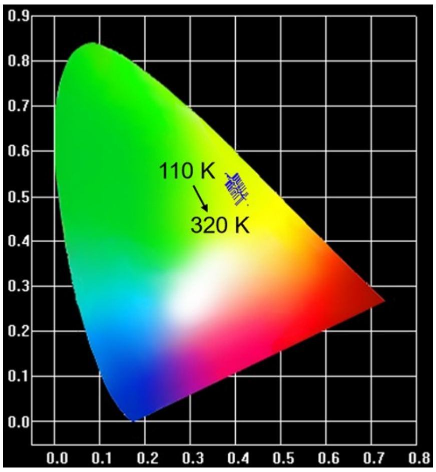

Fig. S20. CIE chromaticity diagram showing the temperature-dependent luminescence color of poly$Eu_{0.0025}Tb_{0.9975}$MOF-$RHP_{80\%}$ membrane.

Table S2. The energy transfer efficiency (*E*) between Tb^{3+} and Eu^{3+} at room temperature was calculated according to previous reported method and listed at Table S2.[7,8]

Eu^{3+}/ Tb^{3+}	8:2	5:5	8:2	0.02:0.98	0.01:0.99	0.005:0.995	0.0025:0.9975
E/%	83.2	83.3	82.1	69.8	69.3	73.8	69.5

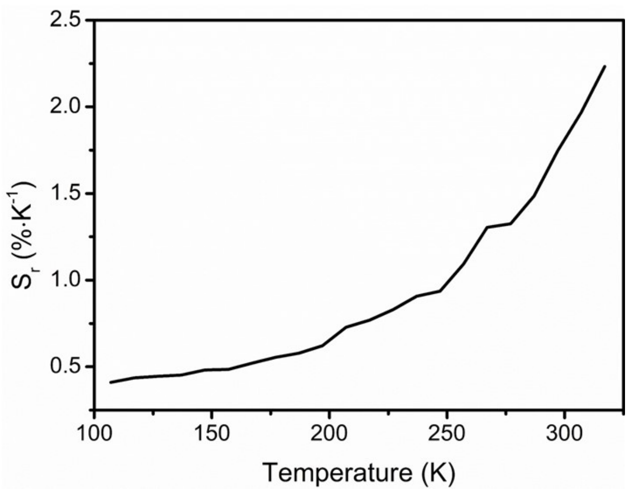

Fig. S21. Relative sensitivity of poly$Eu_{0.0025}Tb_{0.9975}$MOF-$RHP_{80\%}$ membrane.

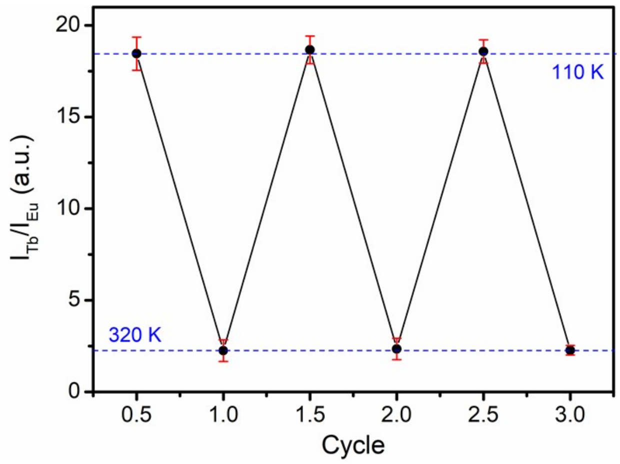

Fig. S22. Temperature cycling between 110 and 320 K for polyEu$_{0.0025}$Tb$_{0.9975}$MOF-RHP$_{80\%}$ membrane revealing a repeatability >99.6%.

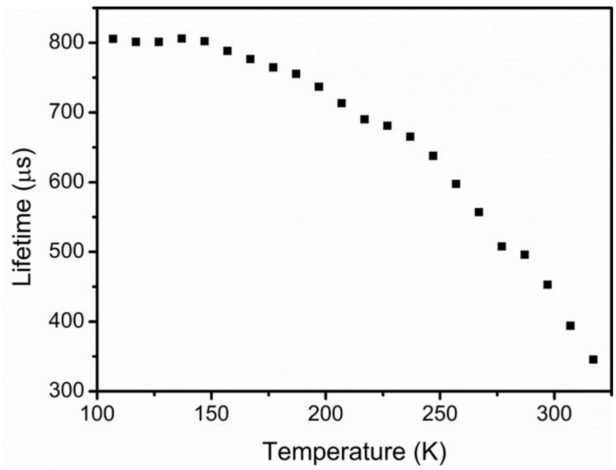

Fig. S23. Temperature dependence of the $^5D_4$ lifetime (110-320 K) for polyTbMOF-RHP$_{80\%}$ membrane. (The decay curves are monitored at 544 nm and excited at 370 nm).

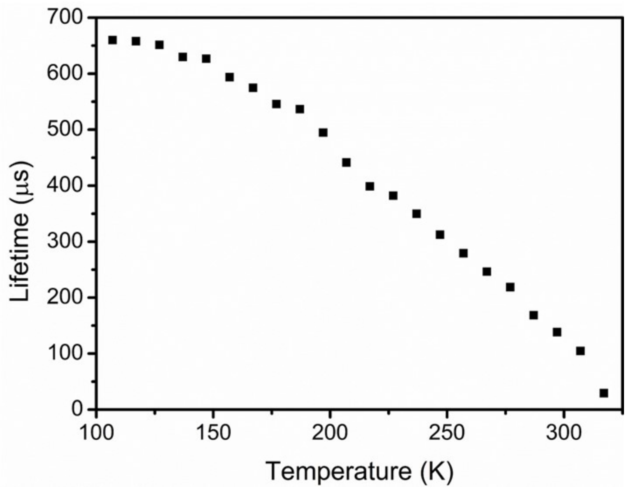

Fig. S24. Temperature dependence of the $^5D_4$ lifetime (110-320K) for poly$Eu_{0.0025}Tb_{0.9975}$MOF-$RHP_{80\%}$ membrane. (The decay curves are monitored at 544 nm and excited at 370 nm).

Table S3. The energy transfer efficiency (E) between Tb^{3+} and Eu^{3+} at different temperature (110-320K).

Temperature/K	*E*/%
107	18.1
117	17.9
127	18.7
137	21.9
147	21.9
157	24.7
167	26.0
177	28.6
187	29.0
197	32.9
207	38.1
217	42.2
227	43.9
237	47.4

247	51.0
257	53.3
267	55.8
277	57.0
287	66.0
297	69.5
307	73.4
317	91.5

3. Supplementary Movie

Movie S1. This movie shows the rapid room-temperature self-healing ability of polyEuMOF-RHP$_{80\%}$ membrane. In general, a rectangle polyLnMOF-RHP$_{80\%}$ sheet (20 × 5 × 1 mm^3) was broken into two pieces by hands, and was brought into contact immediately to heal the damage for 80 s at ~25 °C. As recorded, the healed sheet could readily bear a weight of 500 g.

4. References

1 H. Wang, H. Liu, Z. Cao, W. Li, X. Huang, Y. Zhu, F. Ling, H. Xu, Q. Wu, Y. Peng, B. Yang, R. Zhang, O. Kessler, G. Huang and J. Wu, *Proc. Natl. Acad. Sci. U. S. A.*, 2020, **117**, 11299-11305.

2 M. Xiao and P. R. Selvin, *J. Am. Chem. Soc.*, 2001, **123**, 7067-7073.

3 J. Rocha, C. D. Brites and L. D. Carlos, Chem. Eur. J., 2016, **22**, 14782-14795.

4 D. Ananias, A. D. Firmino, R. F. Mendes, F. A. A. Paz, M. Nolasco, L. D. Carlos and J. Rocha, *Chem. Mater.*, 2017, **29**, 9547-9554.

5 Z. Li, P. Liu, X. Ji, J. Gong, Y. Hu, W. Wu, X. Wang, H.-Q. Peng, R. T. K. Kwok, J. W. Y. Lam, J. Lu and B. Z. Tang, *Adv. Mater.*, 2020, **32**, 1906493.

6 W.-L. Jiang, L.-G. Ding, B.-J. Yao, J.-C. Wang, G.-J. Chen, Y.-A. Li, J.-P. Ma, J. Ji, Y. Dong and Y.-B. Dong, *Chem. Commun.*, 2016, **52**, 13564-13567.

7 Y. Cui, H. Xu, Y. Yue, Z. Guo, J. Yu, Z. Chen, J. Gao, Y. Yang, G. Qian and B. Chen, *J. Am. Chem. Soc.*, 2012, **134**, 3979-3982.

8 X. Rao, T. Song, J. Gao, Y. Cui, Y. Yang, C. Wu, B. Chen and G. Qian, *J. Am. Chem. Soc.*, 2013, **135**, 15559-15564.